

Numerical Investigation on Reducing Fluid Forces Acting on a Square Prism in a Laminar Flow Regime Using a Control Plate

NIDHUL K

Abstract—This paper investigates the passive control of fluid forces acting on a square prism in a laminar flow regime. The passive control employed in this study is a flat plate placed in the upstream of the prism. 2D unsteady numerical simulation is done using FVM employing pressure based solver and PISO scheme in CFD fluent. A computational domain and grid independence study has been carried out to obtain a grid resolution prior to simulation to ensure that there are no discrepancies in the results obtained. The flow Reynolds number based on the square prism side length (D) and inlet flow is chosen as 150. The length of the control plate is chosen as D and the distance between control plate and prism (S) is chosen within the range of $1D-5D$. In this range of S , the different flow patterns and magnitude of reduction of fluid forces are studied and optimal value of S is found out. The results show that the optimal position of control plate is at a distance of $2D$ away from the prism, where almost maximum reduction of fluid forces occurs.

Keywords—Control Plate, Fluid forces, Grid Independence, Laminar Flow, Passive Control, Reynolds number, Square Prism, Vortex shedding.

1 INTRODUCTION

Vortex shedding behind bluff bodies is of concern for many engineering applications. Bluff bodies are structures with shapes that significantly disturb the flow around them, as opposed to flow around a streamlined body. The flow in the wake of a bluff body is unsteady and causes considerable fluctuating forces and can also lead to flow induced vibrations. Fluid flow past a cylindrical object generates vorticity when Re is increased due to the shear present in the boundary layer. This vorticity in the flow field coalesces into regions of concentrated vorticity known as vortices. Further increase of the Reynolds number ($Re > 40$) makes the steady vortices to become unstable and the flow bifurcates to a time-periodic state, in which opposite-signed vortices are periodically shed from the opposite sides of the near wake; this is known as the primary instability of the wake. The periodic vortex shedding generates oscillatory forces on the cylinder. The forces on the plane of the cross-section of the cylinder can be decomposed into drag- the force acting in the same direction of the free-stream - and lift - the force acting in the cross-stream direction. Due to the existence of these oscillatory forces imposed by the flow, flexible cylinders and rigid cylinders mounted on flexible structures vibrate when immersed in a uniform stream.

This vibration occurs predominantly in the cross-stream direction and since the origin of the forces is associated with the vortex shedding, this type of structural response is called vortex-induced vibration (VIV). VIV is a strongly nonlinear phenomenon, since the movement of the cylinder alters the flow field, and the flow field is ultimately responsible for the forces exerted on the cylinder. Vortex shedding is responsible for structural movement of high rise buildings, scour development around bridge piers in channel beds, vibrations of industrial components, acoustic radiation from aircraft landing gear and other related problems. Therefore, it is important to understand and control these flow-induced problems so that engineering design and public comfort can be improved continuously.

The wake and the flow separation can be reduced by flow control methods such as passive, active and compound methods, reducing the unsteadiness and forces acting on the bluff body. Active control methods such as forced fluctuations and jet blowing use external energy to control the flow. Passive control methods control the flow by modifying the shape of the body or by application of a control rod or plate or roughness elements attached or detached to the main body. When Active and passive techniques are applied simultaneously, it is called compound method.

Over the last twenty years, a vast amount of studies has been conducted to increase the understanding of different transition processes of the flow past a circular cylinder- experimentally, numerically and theoretically. By contrast, there are very few similar studies found on flow past rectangular cylindrical structures, e.g. the square prism, at moderate Reynolds number. Inoue et.al [1] constructed a non-uniform mesh but divided the computational domain into three regions, each with a different grid ratio. At Reynolds numbers less than about 500 there is only one single set of experiments,

• Nidhul K is currently working as an Assistant Professor in the Malabar Institute of Technology Kannur, India. E-mail: nidhul07@mail.com

Okajima et al.[2] reported the influence of Reynolds number on the mean drag coefficient. Mohamed Sukri Mat Ali et.al [3] numerically investigated the sensitivity of the computed flow field to flow parameters for a flow with Reynolds number 150. They constructed computational meshes based on reasonable estimates of cell size and grid stretching ratios. S. Ozono [3] conducted experiments over a circular and rectangular cylinder with a horizontal short thin splitter plate below wake centerline and showed that vortex can be suppressed even when the splitter plate is asymmetrically behind the cylinder. Mittal [4] numerically investigated the effect of varying plate length and its position downstream on the near wake of a circular cylinder at a Reynolds number of 100. Slip boundary condition was imposed on the plate, which may not be relevant to practical applications. Rathakrishnan [5] comprehensively studied the vortex shedding suppression using the splitter-plates attached to the end of the cylinder. Zhou et al [6] numerically studied that at low Reynolds numbers, there was reduction in fluid forces acting on a square cylinder (prism) in a two-dimensional channel using a control plate. In this work, a parabolic profile is applied at the channel inlet as compared to a rectangular shaped inlet to minimize the grid size. The control plate height is varied from 0.1-1 times the side length of square cylinder. For each height, the perpendicular distance between the control plate and the cylinder is varied from 0.5 to 3.0 times of the square cylinder width. It was observed that not only the drag on the square cylinder is significantly reduced by the control plate, but also the fluctuating lift was suppressed as well. Doolan [7] numerically studied flow around square cylinder of side length D with a downstream flat plate of length $0.834D$ laid at $2.37D$ from the rear surface of the cylinder. A strong interaction between the shear layers from the square cylinder wall with the flat plate was observed. Mohamed Sukri Mat Ali et.al [8] observed numerically that the critical gap distance G_{cr} for a detached splitter plate is $2.3D$. The plate had no significant effect on the generation of the von Kármán vortex when the separation is beyond $5.6D$. Many studies show that it is very important to accurately obtain the value of G_{cr} as flow transits to a new flow regime after critical gap distance. (e.g., Bull et al. [9]; Carmo et al. [10]; Papaioannou et al. [11]; Zdravkovich [12]). The current study aims to reduce the fluid forces acting on a square prism by the passive control method using a detached flat plate placed in the upstream. The width of the control plate is chosen equal to side length of square prism and its distances from the square prism is varied from $1D$ to $5D$.

2 NUMERICAL SIMULATION PROCEDURE

2.1 Flow Field Formulation

The governing equations on the flow field are the continuity and momentum equations (Navier-Stokes equations), which can be written as follows.

$$\frac{\partial \rho}{\partial t} + \text{div}(\rho V) = 0 \quad (1)$$

$$\frac{\partial}{\partial t}(\rho u) + \text{div}(\rho V u) = -\frac{\partial p}{\partial x} + \text{div}(\mu \text{grad} u) + B_x \quad (2)$$

$$\frac{\partial}{\partial t}(\rho v) + \text{div}(\rho V v) = -\frac{\partial p}{\partial y} + \text{div}(\mu \text{grad} v) + B_y \quad (3)$$

Where ρ is the fluid density, μ is the fluid viscosity, V is the velocity vector of the flow field, p is the pressure, and u and v are the velocity components in the x - and y -directions, respectively. B_x and B_y are also the body forces per unit volume, which are negligible in the present study. The fluid is assumed to be incompressible, and its properties has been taken as $\rho=1.225 \text{ kg/m}^3$ and $\mu=1.7894 \times 10^{-5} \text{ kg/m s}$.

2.2 Limits of the Problem

A rectangular domain was used with a length of $33.5D$ and a width of $20D$, where $D=0.04 \text{ m}$ is side length of the prism as shown in fig.1. The position of the control-plate is varied in the horizontal direction, from the leading edge of the prism in the range $1D$ - $5D$. The control plate length and thickness are D and $0.02D$, respectively.

The fluid flows uniformly (with velocity U_∞) from left to right into the downstream of the domain. Boundary conditions should be enforced at the outlet and the lateral boundaries of the computational domain, as well as on the surfaces of the embedded bodies. At domain inlet and outlet, velocity inlet and pressure outlet respectively have been employed. A symmetry boundary condition at the lateral boundaries of the domain and wall with no-slip condition has been used at the prism wall. On the control plate also no-slip condition has been applied.

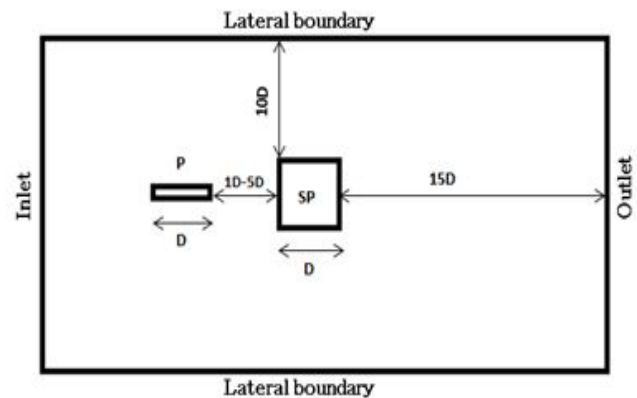


Fig 1: Flow domain for a square prism with a Control plate in the upstream

2.3 Discretization Method

Transforming continuous fluid flow problem into discrete numerical data which are then solved by the computers is known as Discretization. The governing equations have been discretized using the finite-volume method on a fixed Cartesian-staggered grid with non-uniform grid spacing.

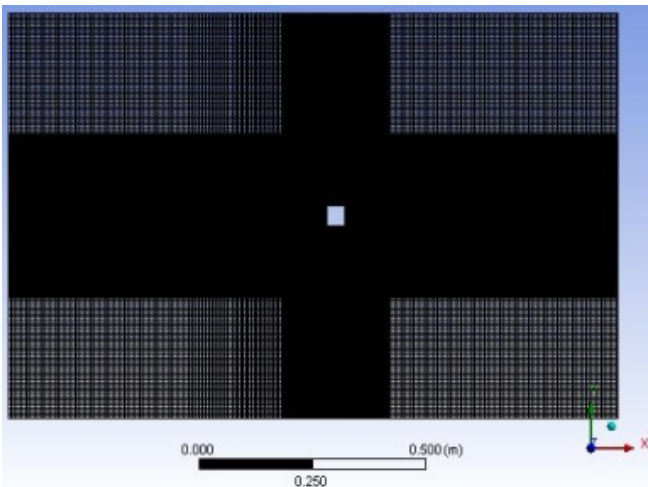


Fig 2: Non-uniform computational grid

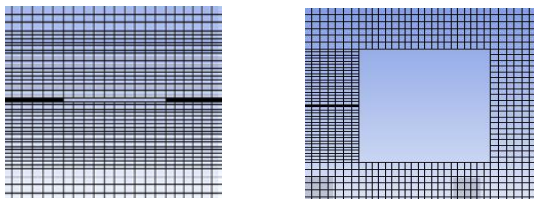


Fig 3: Enlarged view of grid near the control plate and the square prism

The grids in the region of the embedded boundaries are sufficiently fine in order to achieve the reasonable accuracy. The spatial discretization has been performed by using multi-block analysis with structured mesh near both square prism and control plate. The temporal discretization has been done in conformity with the second order implicit scheme. Temporal discretization involves the integration of every term in the differential equations over a time step Δt . The simulations were carried out as an unsteady state with a time step (Δt) size of 0.01 sec with sufficient time steps to achieve results without any discrepancies. A non-uniform grid is made around the square prism and the control plate as shown in fig.2 and fig.3.

2.4 Grid Influence Study

Various numerical studies have been conducted and it's observed that the result comparisons show deviations from accurate value. One of the reasons for these discrepancies is the difference in the construction of the mesh. Generally, the accuracy of a numerical solution increases as the number of cells increases. But employing a larger number of cells requires more computer hardware resource and computing time. So grid independence study has been done so that the grid chosen for simulation provides accurate results and also to optimise the computational resource available. Grid spacing was gradually increased from the prism surface towards the outer boundaries in order to avoid sudden distortion and skewness, and to provide a sufficiently clustered mesh near the prism wall where the flow gradients are large and to capture flow regime within the boundary layer.

Several meshes, with increasing refinement, were tested to ensure that the solution was independent of the mesh. These meshes and the drag coefficient (C_D) predictions are reported in Table 1 at $Re=40$. It is observed that C_D value does not vary much for mesh finer than 81936 cells.

TABLE 1
 Grid independence study for a square prism at $Re = 40$

No. of cells	C_D	% deviation
19100	0.1552	
27504	0.1560	0.537
39364	0.1559	0.102
57050	0.1558	0.063
81936	0.1559	0.006
116640	0.1558	0.075
168139	0.1559	0.003

2.5 Verification of the Solver

Accuracy of the solver is validated in this section by simulation of flow around a square prism. Various parameters such as drag coefficient $C_D = F_D / 0.5\rho u_\infty^2 D$, pressure coefficient $C_p = P - P_{atm} / 0.5\rho u_\infty^2$ and Strouhal number $St = fD / U_\infty$ has been used. Grid independency of the solver has been performed and showed that the results are not sensitive to the grid size. Hereinafter, all the results presented have been obtained with fine grid consisting of 81936 cells. Assuming that this grid provides a sufficient grid-independency for the Reynolds number considered in this paper. The results of the flow around square prism were verified using the dimensionless parameters defined above.

TABLE 2
 Comparison of the Present study at $Re=150$ with other previous studies and experiments

Study	St	C_D	C_L
Experiments(Okajima, 1982; Sohankar et al., 1999)	0.148-0.155	1.40	-
Sohankar et al. (1998)	0.165	1.44	0.230
Doolan (2009)	0.156	1.44	0.296
Inoue et al. (2006)	0.151	1.40	0.40
Ali et al. (2009)	0.160	1.47	0.285
Present study	0.149	1.47	0.179

3 RESULTS AND DISCUSSION

In this work, numerical simulations of the two-dimensional unsteady flow are performed to study the flow around a square prism and forces acting on it due to the flow and effect of placing a control plate in a tandem arrangement for the

laminar regime. The effect of the spacing between the square prism and the control plate ($1D-5D$) are studied for $Re = 150$. Based on this study, the optimum position for the control plate is found out.

3.1 Vortex shedding behind a Square Prism ($Re=150$)

When flow velocity is increased, wake behind the prism becomes unstable. Wake develops a slow oscillation in which the velocity varies periodically with time and downstream distance, with amplitude of oscillation increasing downstream. Oscillating wake rolls up into two staggered rows of vortices with opposite sense of rotation. Because of similarity of the wake with the footprints in a street, staggered row of vortices behind the square prism is called as "Von-Karman Vortex Street". Eddies periodically break off alternately from 2 sides of the prism as shown in fig.4. While an eddy on one side is shed, that on the other side forms resulting in an unsteady flow near the prism. As vortices of opposite circulations are shed off alternately from 2 sides of the prism, results in an oscillating "lift" or lateral force.

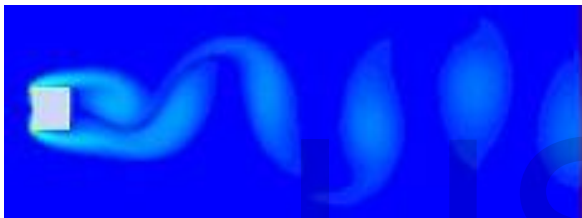


Fig 4: Vorticity magnitude contour in the wake of a square prism

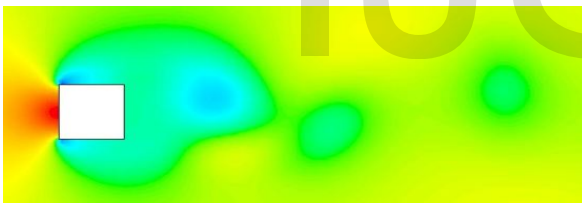


Fig 5: Static pressure contour for a Square prism (in the vicinity of Square prism)

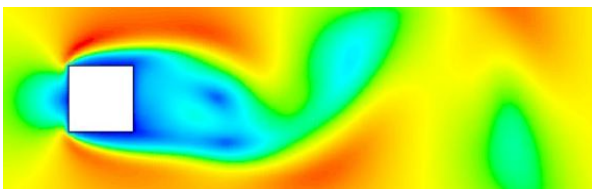


Fig 6: Velocity magnitude contour for a square prism (in the vicinity of Square prism)

Static pressure contour shown in fig.5 shows the static pressure distribution near the prism highlighting the stagnation point and the velocity magnitude contour shown in fig.6 indicates the retardation of fluid layers adjacent to the solid boundary due to no-slip condition and fluid layers form ed-

dies in the immediate vicinity of the wake due to reduction in velocity combined with adverse pressure gradient

3.2 Effect of control plate on Vortex shedding and flow characteristics for a Square Prism

Simulation was performed for a Square Prism at $Re=150$ with a detached Control plate of constant thickness in the upstream of the prism at varying gap distance $1D \leq S \leq 5D$. The vorticity magnitude contours for each gap distance was obtained as shown in fig.7.

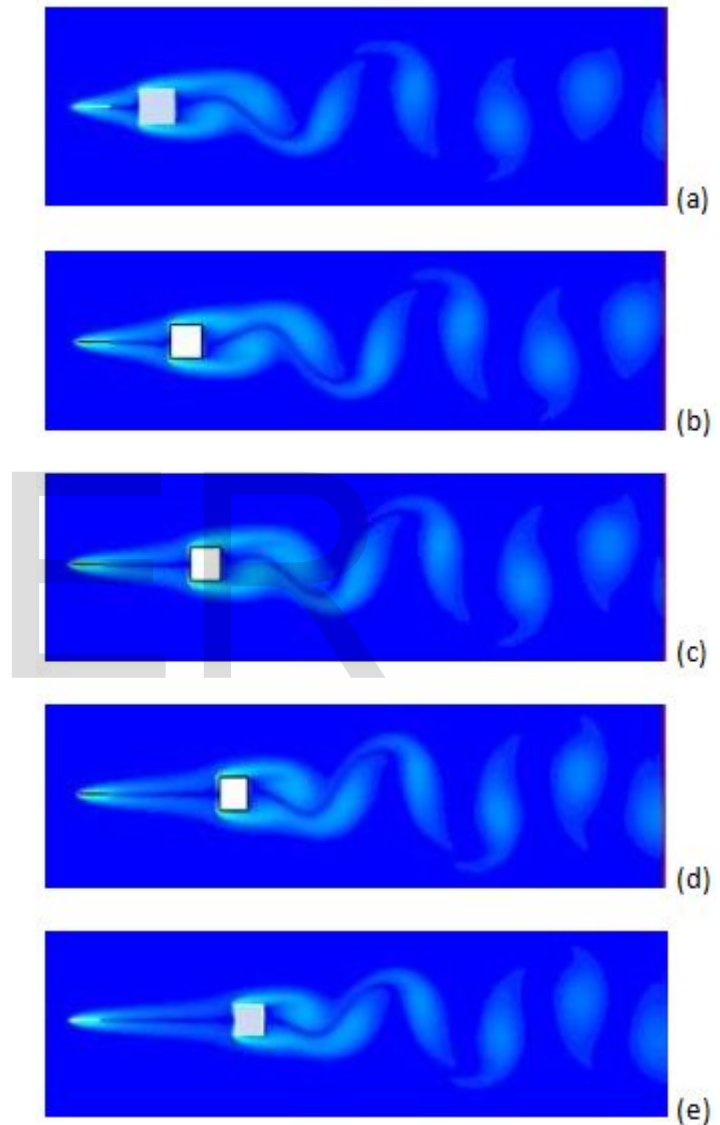


Fig 7: Vorticity magnitude contour in the wake of a square prism with an upstream control plate (a) $S=1D$ (b) $S=2D$ (c) $S=3D$ (d) $S=4D$ (e) $S=5D$

It is observed that with an upstream control plate at $S=1D$ and $S=2D$, the first pair of vortices get stretched when compared to flow over a square prism without control plate. Beyond $S=2D$, there is no stretching. The variation of Strouhal number with gap distance is shown in fig.8. It is observed that St increases for $S=1D$ and then gradually decreases for the

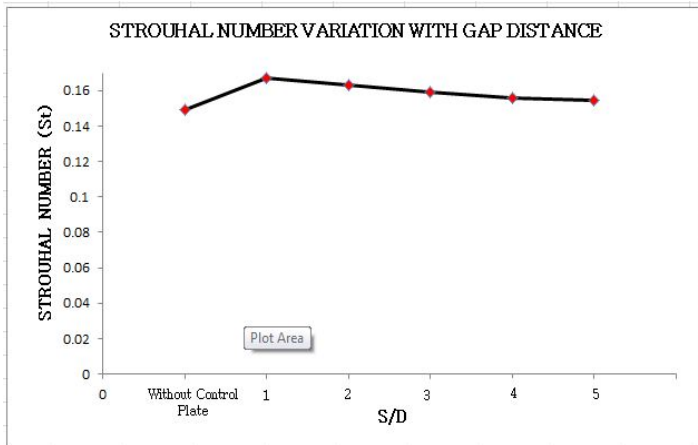


Fig 8: Strouhal number variation for varying gap distance (s)

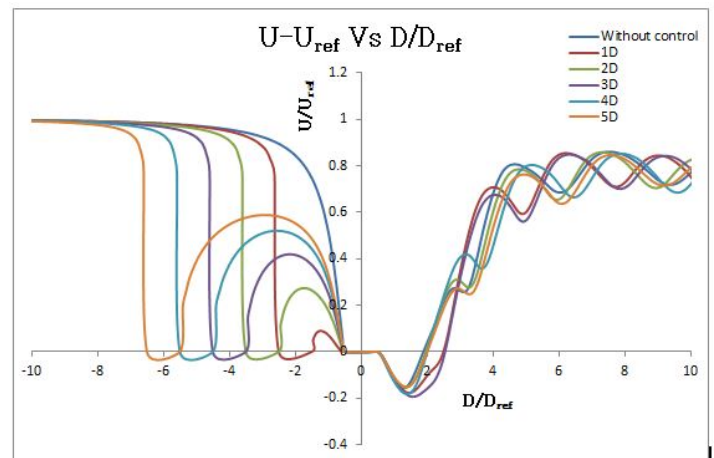


Fig 10: U/U_{ref} Vs D/D_{ref}

increasing values of S . This is due to blockage effect created by the plate which reduces convective speed of the fluid shear layers. However the effect slowly weakens as gap distance further increases. The same is also observed from the velocity magnitude contours as shown in fig 9. For $S > 2D$, the presence of control plate does not reduce the speed of shear layers as much as in that for $S=1D$ and $S=2D$. U/U_{ref} graph shown in fig 10 also depicts the same.

Apart from velocity profile, pressure distribution is an important parameter in the study of flow around a square prism. Pressure changes accordingly with the vortices motion in the vicinity of the body. At stagnation point, located at midpoint of face 1-2 as shown in fig 11, flow comes to rest and pressure reaches a maximum value.

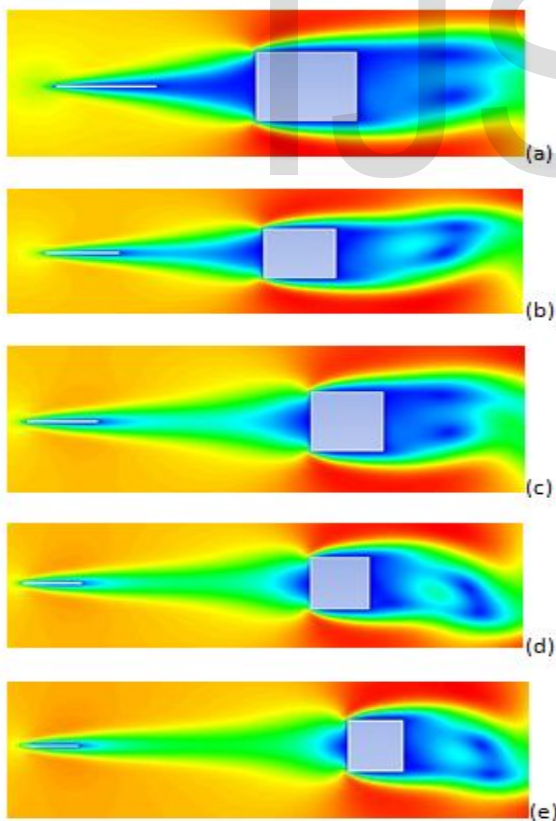


Fig 9: Velocity magnitude contour for a square prism with an upstream control plate (a) $S=1D$ (b) $S=2D$ (c) $S=3D$ (d) $S=4D$ (e) $S=5D$

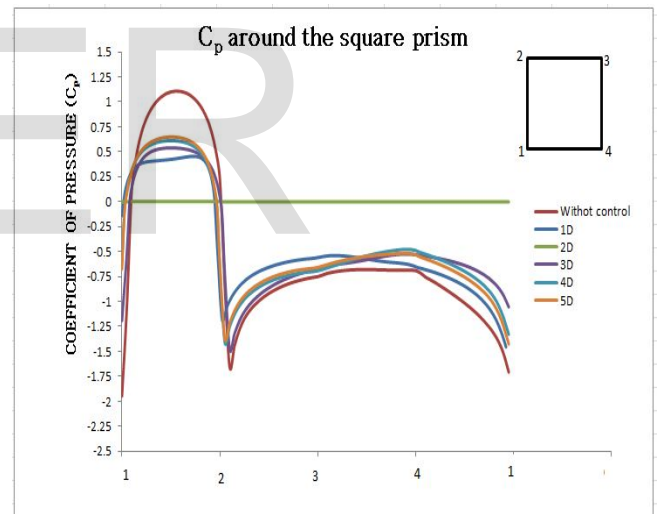


Fig 11: Coefficient of pressure variation along the prism surface

It is observed that in case of square prism without control plate, the adverse pressure gradient is higher. Pressure fluctuations are least in the case when $S=2D$. This is also observed from the variation of coefficient of pressure in the wake region as shown in fig 12.

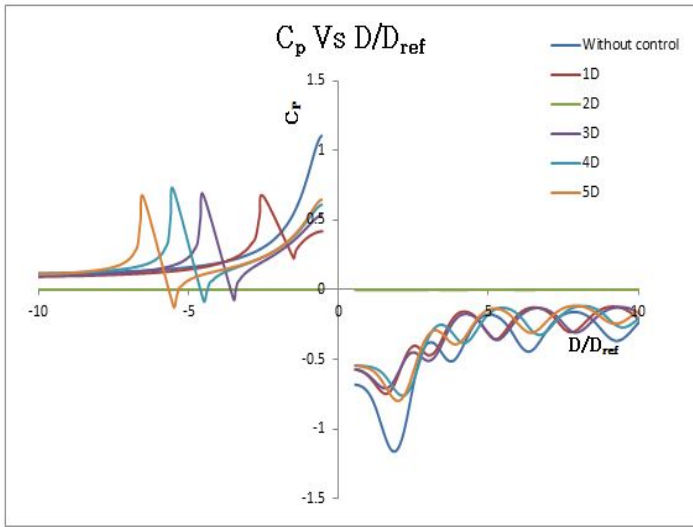


Fig 12: Coefficient of pressure variation along the prism surface

The variation of Coefficient of drag with varying gap distance is shown in fig 13. It is observed that drag force is lower when the control plate is kept at a distance of $S=2D$ as compared

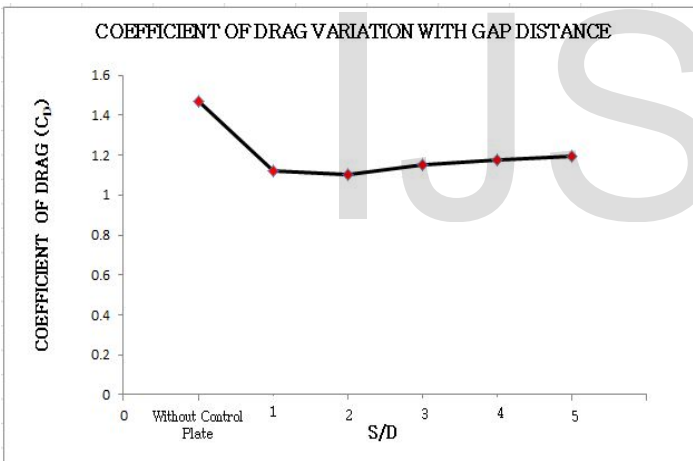


Fig 13: Coefficient of Drag variation for varying gap distance

to square prism with no control plate. The percentage reduction in drag is shown in table 3.

TABLE 3

Comparison of the Present study at $Re=150$ with other previous studies and experiments

S/D	1	2	3	4	5
% REDUCTION IN C_D	23.913	25.250	21.6209	20.080	18.847

The variation of Coefficient of lift with varying gap distance

is shown in fig 14. It is observed that lift force is lower when the control plate is kept at a distance of $S=2D$ as compared to square prism with no control plate.

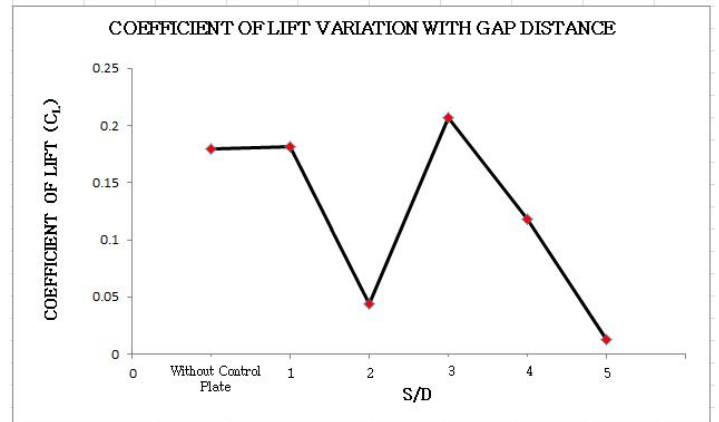


Fig 14: Coefficient of Lift variation for varying gap distance

4 CONCLUSION

In this paper, the effect of placing a control plate upstream of a Square prism has been studied to reduce the fluid forces acting on the prism in a laminar flow regime ($Re = 150$).

An upstream control plate reduces the flow induced forces by interrupting the regular vortex shedding. The pressure field and velocity field in the flow over a square prism depends on the control plate position upto a certain gap distance where the effect is noticeably felt. For a gap distance of $S=2D$, the adverse pressure gradient is much smaller and the velocity of shear layers is more compared to other gap distance. Also the flow induced forces namely drag force and lift force is lower for $S=2D$. There is a reduction of 25% in C_D when the control plate is placed at $S=2D$ when compared to that of flow over a square prism with no control plate. Hence the optimum gap distance for this configuration under study is obtained as $S=2D$.

REFERENCES

- [1] Inoue, Iwakam, and Hatakeyama (2006). "Aeolian tones radiated from flow past two square cylinders in a side-by-side arrangement" *Physics of Fluids*, 18(4), 046104.
- [2] Okajima, A., 1982, *Strouhal numbers of rectangular cylinders*. *Journal of Fluid Mechanics* 123, 379–398.
- [3] Ozono, S., 1999. *Flow control of vortex shedding by a short splitter plate asymmetrically arranged downstream of a cylinder*. *Physics of Fluids* 11, 2928–2934.
- [4] Mittal, S., 2003. *Effect of a "slip" splitter plate on vortex shedding from a cylinder*. *Physics of Fluids* 15, 817–820.
- [5] Rathakrishnan, E., 1999, "Effect of Splitter-Plate on Bluff body Drag" *AIAA Journal*, 37(9), pp. 1125–1126.

[6] Zhou, L., Cheng, M., Hung, K.C., 2005. Suppression of fluid force on a square cylinder by flow control. *Journal of Fluids and Structures* 21, 151–167.

[7] Doolan, C.J., 2009. *Flat-plate interaction with the near wake of a square cylinder*. *AIAA Journal* 47, 475–478.

[8] Mohamed Sukri Mat Ali , Con J. Doolan & Vincent Wheatley, 2012, "Low Reynolds number flow over a square cylinder with a detached flat plate", *International Journal of Heat and Fluid Flow*, *International Journal of Heat and Fluid Flow* 36 (2012) 133–141.

[9] Bull, M.K., Blazewicz, A.M., Pickles, J.M., Bies, D.A., 1996. *Interaction between a vortex wake and an immersed rectangular plate*. *Experimental Thermal and Fluid Science* 12, 209–220.

[10] Carmo, B.S., Meneghini, J.R., Sherwin, S.J., 2010. *Secondary instabilities in the flow around two circular cylinders in tandem*. *Journal of Fluid Mechanics* 644, 395–431.

[11] Papaioannou, G.V., Yue, D.K.P., Triantafyllou, M.S., Karniadakis, G.E., 2006. *Three dimensionality effects in flow around two tandem cylinders*. *Journal of Fluid Mechanics* 558, 387–413.

[12] Farhadi, M., Sedighi, K., Fattahi, E., 2010. *Effect of a splitter plate on flow over a semi-circular cylinder*. *Proceedings of the Institution of Mechanical Engineers, Part G: Journal of Aerospace Engineering* 224, 321–330.

[13] Zdravkovich, M.M., 1987. *The effects of interference between circular cylinders in cross flow*. *Journal of Fluids and Structures* 1, 239–261.

[14] Behzad Ghadiri Dehkordi and Hamed Hourijafari 2010, *On the Suppression of Vortex Shedding From Circular Cylinders Using Detached Short Splitter-Plates*. *Journal of fluids Engineering, April (2010) Vol. 132 / 044501-1*.

[15] Sohankar, A., Norberg, C., Davidson, L., 1999. *Simulation of three-dimensional flow around a square cylinder at moderate Reynolds numbers*. *Physics of Fluids* 11, 288–306.